

An Equivalent Site Mechanism for Na⁺ and K⁺ Binding to Sodium Pump and Control of the Conformational Change Reported by Fluorescein 5'-Isothiocyanate Modification[†]

Irina N. Smirnova, Shwu-Hwa Lin, and Larry D. Faller*

Center for Ulcer Research and Education, Department of Medicine, University of California at Los Angeles School of Medicine, and Wadsworth Division, Department of Veterans Affairs Medical Center, West Los Angeles, California 90073

Received March 2, 1995; Revised Manuscript Received April 27, 1995[®]

ABSTRACT: We have previously shown that two K⁺ must bind to cause the conformational change in Mg²⁺-dependent and Na⁺- and K⁺-stimulated ATPase reported by fluorescein 5'-isothiocyanate modification and that the ratio of the macroscopic K⁺ dissociation constants is 4 [Smirnova, I. N., & Faller, L. D. (1993) *J. Biol. Chem.* 268, 16120–16123]. Since 4 is the ratio expected for random binding to two identical and independent sites, in this paper we propose a two-equivalent-site mechanism for Na⁺ as well as K⁺ binding to sodium pump and control of the conformational change between E₁ and E₂. The equivalent site mechanism is tested by fitting algebraic equations for the empirical first-order rate constant and for the magnitude of the fluorescence change observed in stopped-flow experiments to an array of data. The estimated rate constants for the conformational change at 15 °C are $k_f = 150 \pm 19 \text{ s}^{-1}$ and $k_r = 0.13 \pm 0.03 \text{ s}^{-1}$, and the estimated dissociation constants for K⁺ and Na⁺ from the E₁ conformation of the enzyme are $K_K = 4.8 \pm 1.2 \text{ mM}$ and $K_{Na} = 0.38 \pm 0.12 \text{ mM}$, in good agreement with estimates from published binding measurements. Although the possibility of ordered and anticooperative binding cannot be excluded, the equivalent site interpretation is supported by quasi-independent estimates of the macroscopic Na⁺ dissociation constants that give the ratio 4 predicted for binding to identical, noninteracting sites and by equivalent site interpretations of published transport experiments. Six alternative mechanisms are tested. Noncompetitive binding and mutually exclusive binding of the transported ions can be ruled out. Comparable fits to the data are obtained by three-equivalent-site mechanisms in which enzyme with either two or three K⁺ bound can undergo the conformational change. Therefore, this study quantitatively supports the conformational hypothesis by showing that a conformational change in sodium pump has the right properties to explain transport.

The seminal idea in the sodium pump field is that conformational changes play a crucial role in the physical translocation of ions by the enzyme. There is convincing evidence for different conformations of the protein. However, experiments designed to test the conformational hypothesis more rigorously by demonstrating that a conformational change has the right properties to participate in transport have been only partially successful. The starting point for this paper was the discrepancy in the literature between the stoichiometry of ion transport and the stoichiometry of ion-induced conformational changes reported by extrinsic fluorescent probes of protein structure. Resolution of the discrepancy has led to formulation of a new mechanism for ion binding and control of a conformational change that quantitatively supports the conformational hypothesis.

The consensus is that two K⁺ are transported in exchange for three Na⁺ per molecule of ATP¹ hydrolyzed by Na,K-ATPase (Glynn, 1984). This conclusion is generally sup-

ported both by direct measurements of ion binding (Glynn, 1985) and by measurements of ion occlusion (Glynn & Karlsh, 1990). *A priori* the ions could be translocated either sequentially or simultaneously. The latter interpretation is favored by transport measurements. For example, sigmoidal dependence of the rate of active K⁺ influx into red blood cells on external [K⁺] indicates either that two sites must be filled for transport to occur or that one site must be occupied by two K⁺ (Sachs & Welt, 1967). Therefore, the prediction following from transport studies is that the conformational change involved in ion movement does not occur until two K⁺ are bound. An experimentally testable corollary is that a rate-limiting conformational change depends sigmoidally on [K⁺].

A slow conformational change reported by intrinsic fluorescence is accelerated by ATP (Karlsh & Yates, 1978), consistent with the prediction from studies of the catalytic cycle that there is an "occluded" conformation of the unphosphorylated enzyme (Post *et al.*, 1972). Conformational changes with a comparably slow rate that are reported by reversible binding of FDP (Karlsh *et al.*, 1978) or by chemical modification of sodium pump with either FITC (Karlsh, 1980; Shani-Sekler *et al.*, 1988) or IAF (Steinberg & Karlsh, 1989) have been studied as a function of [K⁺]. In every case the empirical first-order rate constant depended either linearly or hyperbolically on [K⁺], so there was no evidence that more than one K⁺ is required to cause the conformational change. This unexpected result was rational-

[†] This work was supported by grants DK36873 from the U.S. Public Health Service and MCB9106338 from the National Science Foundation and by a Veterans Administration Merit Review Award.

[®] Abstract published in *Advance ACS Abstracts*, June 15, 1995.

¹ Abbreviations: Na,K-ATPase, Mg²⁺-dependent and Na⁺- and K⁺-stimulated ATPase (EC 3.6.1.37); ATP, adenosine 5'-triphosphate; FITC, fluorescein 5'-isothiocyanate (isomer 1); IAF, 5-(iodoacetamido)-fluorescein; FDP, formycin diphosphate; ChoCl (Cho⁺Cl⁻), choline chloride; EDTA, ethylenediaminetetraacetic acid; SDS, sodium dodecyl sulfate; Tris (Tris⁺), tris(hydroxymethyl)aminomethane.

ized by assuming that there are "high-" and "low-affinity" K^+ sites and that the conformational change does not occur until the lower affinity site is filled (Karlsh & Stein, 1985). Analogous reasoning has been used to interpret "strictly hyperbolic" Rb^+ occlusion curves as evidence for a site with 3 orders of magnitude higher affinity for Rb^+ than the site that triggers the conformational change (Shani *et al.*, 1987).

However, the *ad hoc* assumption of an experimentally silent, high-affinity K^+ site does not explain a quantitative discrepancy of more than 1 order of magnitude between the half-maximum $[K^+]$ observed when FITC-enzyme is titrated with K^+ experimentally and the $K_{0.5}$ predicted for equilibrium titrations from kinetic parameters, if only one fluorometrically detectable site is assumed (Faller *et al.*, 1991). Therefore, we extended kinetic titrations of FITC-labeled sodium pump to lower K^+ concentrations than reported in earlier studies and demonstrated that the empirical first-order rate constant for the conformational change depends sigmoidally on $[K^+]$ (Smirnova & Faller, 1993b). Numerical estimates of macroscopic K^+ dissociation constants that correctly predict the half-maximum $[K^+]$ in equilibrium titrations were obtained from the concentration dependence of the empirical first-order rate constant by assuming that two K^+ must bind before the conformational change occurs. Therefore, the K^+ -induced conformational change reported by FITC modification of sodium pump can be explained by a mechanism that is consistent with the prediction of transport studies and would explain the stoichiometry of K^+ transport.

The values estimated for the K^+ dissociation constants entail a new interpretation of K^+ binding and suggest a mechanism for the conformational change. The first K^+ binds 4 times tighter than the second, refuting the claim that there are two sites differing in affinity for K^+ by several orders of magnitude. The observed ratio of the macroscopic K^+ dissociation constants is consistent either with ordered and anticooperative binding to one or two sites with microscopic dissociation constants differing 4-fold or with random binding to two equivalent and noninteracting sites. The latter interpretation is intriguing because there is precedent for conformational changes in other proteins, including ligand-gated channels (Changeux, 1990), resulting from independent binding to several sites followed by a concerted transition (Monod *et al.*, 1965).

Sigmoidal dependence of the conformational change reported by eosin on $[Na^+]$ has been observed and interpreted as evidence for more than one Na^+ site (Skou & Esmann, 1983; Esmann, 1994). However, the conclusion drawn from published data on reversal of the K^+ -induced conformational change in FITC-modified Na,K-ATPase by Na^+ is inconsistent with the transport stoichiometry, attributing reversal to competition between Na^+ and K^+ for a single site (Karlsh, 1980). If, as we have shown, two K^+ control the conformational change reported by fluorescein and Na^+ binds competitively, then it should be possible to demonstrate that more than one Na^+ binds, and if K^+ binds randomly to two identical and independent sites, then a ratio of 4 is predicted for the Na^+ dissociation constants, as well as for the K^+ dissociation constants. We have published preliminary data indicating that binding of at least two Na^+ is required to explain reversal of the conformational change in FITC-enzyme caused by K^+ and that Na^+ reversal experiments are also compatible with random binding to two equivalent and noninteracting sites (Faller *et al.*, 1994).

In this paper we propose an equivalent site mechanism for Na^+ and K^+ binding to sodium pump and control of the conformational change in unphosphorylated enzyme. We

derive algebraic equations for the experimentally observed first-order rate constant and for the amplitudes of K^+ quench and Na^+ reversal experiments from the chemical equation. We test the mechanism by showing that an array of data in which the dependent variables have been measured as functions of $[K^+]$ and $[Na^+]$ reproduces all the predicted features of the mechanism and can be fit by the algebraic equations with a single set of empirical parameters. We exclude several alternative mechanisms by comparing their predictions with what is observed experimentally. Finally, we discuss whether the proposed equivalent site mechanism is a unique explanation of our data and whether the conformational changes in sodium pump reported by other extrinsic fluorophores can be explained by the same mechanism.

EXPERIMENTAL PROCEDURES

Materials

FITC-Labeled Enzyme. Membrane fragments containing Na,K-ATPase were isolated from pig kidneys and labeled with FITC. The procedures we used to purify and chemically modify the enzyme were described in the first paper in this series on the conformational change reported by FITC labeling (Faller *et al.*, 1991). More than one amino acid in Na,K-ATPase reacts with FITC (Xu, 1989), but we have shown that the different reactions reported by fluorescein are temporally resolved in a stopped-flow experiment (Lin & Faller, 1993) and that only the conformational change reported by fluorescein at ATP-protectable, antibody-inaccessible sites (Abbott *et al.*, 1991) is observed, if there is no change in ionic strength (μ). The maximum percentage change in fluorescence depends on the efficiency of labeling the site that reports the conformational change compared to nonspecific labeling and varied from 8% to 12% in the reported experiments. The standard error in the maximum rate estimated for the five different enzyme preparations was $\pm 5\%$.

Reagents. Fresh pig kidneys were a gift from Farmer John Clougherty Packing Co. (Los Angeles, CA). FITC (isomer 1) was purchased from Molecular Probes Inc. (Eugene, OR), and the chloride salts of choline, potassium, and sodium were purchased from Sigma (St. Louis, MO). All other reagents were the highest grade commercially available.

Methods

Stopped-Flow Measurements. The instrument we used to make stopped-flow measurements was also described in an earlier paper in this series (Smirnova & Faller, 1993a), and critical experimental considerations like the dead-time (t_d) of the instrument have been discussed (Faller *et al.*, 1994). All of the data reported in this paper were obtained in 50 mM Tris-HCl buffer at pH 7.4 and 15 °C with $\mu \approx 250$ mM. The independent variables are $[K^+]$ and $[Na^+]$. The concentration of either ion may be fixed in a "quench" or "reversal" experiment. In a quench experiment, K^+ is mixed with enzyme $\pm Na^+$ and a decrease in fluorescence is observed experimentally. In a reversal experiment, Na^+ is mixed with enzyme previously quenched by K^+ resulting in an increase in fluorescence intensity, or fluorescence enhancement. The reason the fluorescence must be quenched by K^+ before the reversal reaction can be observed is that the enzyme is in the conformation with higher fluorescence intensity in the selected combination of buffer and μ (Lin &

Faller, 1993). Whenever possible, the experiments were designed so that μ did not change significantly when the enzyme and reagent solutions were mixed, that is, the contents of the enzyme and reagent syringes were identical except for 0.13 mM Tris-EDTA from the purification and labeling procedures in the enzyme solution, the reactants, and ChoCl which was varied so that the sum of the added salt (NaCl, KCl, and ChoCl) concentrations in each syringe equaled 200 mM. In a few experiments, we took advantage of the fact that the slow conformational change can be temporally resolved from faster fluorescence changes caused by an ionic strength jump in order to extend the Na^+ concentration range, or vary $[\text{Na}^+]$ and quench with 100 mM K^+ (final). In these experiments the $[\text{ChoCl}]$ in the enzyme syringe was adjusted so that the contribution of added salts to μ from both syringes equaled 200 mM after mixing. The concentration of enzyme was never more than a few percent of either monovalent cation concentration, so the free metal ion concentration can be equated with the total added metal ion concentration in calculations. Specific protocols for each type of experiment are given in the figure legends.

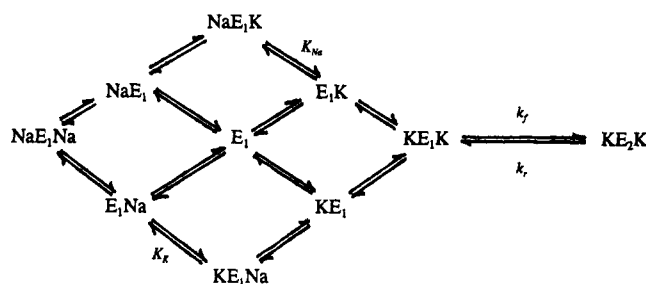
Data Analysis. The dependent variables are the empirical first-order rate constant, which can be treated as a reciprocal relaxation time (τ), and the magnitude of the observed fluorescence change (ΔF). Both time constant and amplitude were estimated from the same recording of voltage, which is proportional to fluorescence intensity, versus time by nonlinear least-squares fits of the equation for an exponential decay (quench experiment) or an exponential increase (reversal experiment) to the data. The observed amplitudes were corrected for the instrument t_d (Faller *et al.*, 1991), and the corrected fluorescence changes (ΔF_o) are plotted in the figures as percentages of the final voltage or fluorescence intensity (F). Scatter plots of the mean experimental data points \pm standard deviation are shown in the figures.

Alternative mechanisms to explain the data were tested by deriving algebraic equations for the concentration dependence of the dependent variables. The parameters were estimated by fitting the equation for $1/\tau$ to the data with the nonlinear least-squares curve fit program in SigmaPlot 5.01, which permits global fits to an array of data. The best strategy for estimating each parameter depends on its numerical value, as well as the functional form of the relaxation expression, and is illustrated in the Results section for the simplest mechanism consistent with our experimental observations. We also explain in the Results section why parameters were not estimated from amplitude data. The compatibility of equilibrium (ΔF_o) data with kinetic ($1/\tau$) data is shown either by generating theoretical curves with parameter estimates from $1/\tau$ data and the transform utility in SigmaPlot 5.01 or by fitting amplitude data with some of the parameters constrained to values estimated from kinetic data. In the text, estimated parameter values are differentiated from parameter values imposed as constraints by quoting the standard deviation in the estimated values. The criteria used to discriminate among alternative mechanisms were, first, whether a mechanism correctly predicts the shapes of the titration curves, second, whether both kinetic and equilibrium data from different types of experiments can be fit with a single set of parameter values, and, third, the relative quality of the fits as judged by the residual sum of squares and the number of runs in residual plots.

Theory

Mechanism. Mechanism 1, in which the conformational change is assumed to be rate-limiting, is the simplest chemical equation that can be written to explain sigmoidal dependence of both $1/\tau$ for the quench reaction on $[\text{K}^+]$ (Smirnova & Faller, 1993b) and ΔF_o for the reversal reaction on $[\text{Na}^+]$ (Faller *et al.*, 1994).

Mechanism 1



E_1 denotes the conformation of FITC-enzyme with higher fluorescence intensity. The principal assumption in the proposed mechanism is that binding occurs randomly to two identical and independent sites for which K^+ and Na^+ compete. The bound ion is written on the left or right simply as a convenience in keeping track of microscopic enzyme forms that are not distinguishable experimentally, like the hybrid species NaE_1K and KE_1Na . The number of microscopic enzyme forms, or ways of filling the available sites with specified numbers of two different ligands, is given by eq 1,

$$\omega_{ij} = \frac{n!}{i!j!(n-i-j)!} \quad (1)$$

where n is the number of sites, i is the number of bound Na^+ , and j is the number of bound K^+ (Edsall & Wyman, 1958). Arbitrarily defining from left to right as the forward direction, the reaction is described by four experimentally determinable parameters, the forward (k_f) and reverse (k_r) rate constants for the conformational change and two microscopic dissociation constants. K_K and K_{Na} are the intrinsic dissociation constants of K^+ and Na^+ , respectively, from either of the equivalent and noninteracting sites on the E_1 conformation of the enzyme. For simplicity we have omitted a number on the left in the subscript of the dissociation constants that was used in our earlier publications to indicate the enzyme conformation, because only Na^+ and K^+ binding to the E_1 conformation is considered in the proposed mechanism.

Algebraic Equations. Algebraic equations for the dependent variables were derived by the method described previously (Smirnova & Faller, 1993a). Equation 2 is the relaxation expression for both K^+ quench (forward) and Na^+ reversal (reverse) reactions.

$$\frac{1}{\tau} = k_f \left[\frac{[\text{K}^+]}{[\text{K}^+] + K_K \left(1 + \frac{[\text{Na}^+]}{K_{Na}} \right)} \right]^2 + k_r \quad (2)$$

The subscript o used in earlier publications to denote total $[\text{K}^+]$ has been dropped to avoid confusion with K^+ outside. Equation 3 gives the $[\text{K}^+]$ at which half the observed change in $1/\tau$ occurs when $[\text{K}^+]$ is chosen as the independent variable.

$$[K^+]_{1/2} = K_K \left(1 + \frac{[Na^+]}{K_{Na}} \right) (1 + \sqrt{2}) \quad (3)$$

Equation 4 is the corresponding expression for the alternative choice of independent variable.

$$[Na^+]_{1/2} = K_{Na} \left[1 + \frac{[K^+]}{K_K} \right] (\sqrt{2} - 1) \quad (4)$$

The observed amplitude can always be calculated with eq 5

$$\Delta F_o = [\chi_{KE_2K}(\text{initial}) - \chi_{KE_2K}(\text{final})] \Delta F_{\max} \quad (5)$$

in which $\chi_{KE_2K}(\text{initial})$ is the fraction of the enzyme in the E_2 conformation at the initial Na^+ and K^+ concentrations before mixing, $\chi_{KE_2K}(\text{final})$ is the fraction of the enzyme in the E_2 conformation when equilibrium is reached at the final $[Na^+]$ and $[K^+]$ after mixing, and ΔF_{\max} is the difference in fluorescence intensity between the E_1 and E_2 conformations. Most of the experiments that will be reported are two limiting cases of eq 5 for which more explicit equations can be derived. If $[K^+]_{\text{initial}} = 0$ in a quench experiment, which assures that the enzyme is initially in the E_1 conformation because of our choice of buffer and μ , the change in fluorescence is given by eq 6

$$-\Delta F_o = \left\{ \left[[K^+]^2 \left[[K^+]^2 + \frac{2K_K}{(1+K_c)} \left(1 + \frac{[Na^+]}{K_{Na}} \right) [K^+] + \frac{K_K^2}{(1+K_c)} \left(1 + \frac{[Na^+]}{K_{Na}} \right)^2 \right] \frac{K_c}{(1+K_c)} \right] \right\} \Delta F_{\max} \quad (6)$$

where $K_c = k_i/k_r$ and the general expression for χ_{KE_2K} is enclosed in braces. For a reversal experiment in which $[Na^+]_{\text{initial}} = 0$ and $[K^+]_{\text{initial}} = [K^+]_{\text{final}}$, eq 7 gives the fluorescence change.

$$\Delta F_o = \left\{ \left[[Na^+]^2 + 2K_{Na} \left(1 + \frac{[K^+]}{K_K} \right) [Na^+] \right] \left[[Na^+]^2 + 2K_{Na} \left(1 + \frac{[K^+]}{K_K} \right) [Na^+] + K_{Na}^2 \left(1 + \frac{[K^+]}{K_K} \right)^2 + \frac{K_c [K^+]^2}{K_K^2} \right] \right\} \left\{ [K^+]^2 \left[[K^+]^2 + \frac{2K_K}{(1+K_c)} [K^+] + \frac{K_K^2}{(1+K_c)} \right] \right\} \frac{K_c}{(1+K_c)} \Delta F_{\max} \quad (7)$$

Assuming that all of the theoretically possible change in fluorescence $[K_c \Delta F_{\max} / (1 + K_c)]$ can be observed in a titration, eq 8 gives the half-maximum concentration for the choice of $[K^+]$ as independent variable in either a quench or reversal experiment.

$$[K^+]_{1/2} = K_K \left(1 + \frac{[Na^+]}{K_{Na}} \right) \left(\frac{1 + \sqrt{2 + K_c}}{1 + K_c} \right) \quad (8)$$

Equation 9 is the corresponding expression for either a reversal or quench experiment, if $[Na^+]$ is chosen as the independent variable.

$$[Na^+]_{1/2} = K_{Na} \left[\sqrt{2 \left(1 + \frac{[K^+]}{K_K} \right)^2 + \frac{K_c [K^+]^2}{K_K^2}} - \left(1 + \frac{[K^+]}{K_K} \right) \right] \quad (9)$$

Titration curves that go through a maximum may be observed if the fixed $[Na^+]$ is not high enough to completely reverse the quench in a reversal experiment when $[K^+]$ is varied or if $[K^+]_{\text{initial}} \neq 0$ and $[Na^+]$ is the independent variable in a quench experiment. In principle, the maximum in the curve can be found by setting the derivative of the appropriate amplitude equation with respect to the independent variable equal to zero. In practice, biquadratic equations are obtained that are intractable. Any of the equations can be rewritten in terms of macroscopic dissociation constants for one or both of the ions with the help of the statistical relationship between the microscopic constant (denoted by upper case K to avoid confusion with rate constants) and the macroscopic constants (indicated by numerical subscripts) for random dissociation from two equivalent and noninteracting sites (Edsall & Wyman, 1958).

$$K = 2K_1 = \frac{K_2}{2} \quad (10)$$

Predictions. The theoretical curves in Figure 1 were calculated with published parameter estimates (Smirnova & Faller, 1993b; Faller *et al.*, 1994). Figure 1a shows the expected variation of $1/\tau$ in either a quench or reversal experiment as a function of $[K^+]$ and $[Na^+]$ calculated with eq 2. Figure 1b is the absolute value of the predicted amplitude in a quench experiment described by eq 6, and Figure 1c is the corresponding plot of the predicted amplitude in a reversal experiment calculated with eq 7. Experiments have been designed to test each of the predictions illustrated in Figure 1.

RESULTS

Quench: $1/\tau, \Delta F_o = f([K^+])_{[Na^+]}$. In this type of quench experiment $[Na^+]$ is fixed and $[K^+]$ is varied. According to eq 2, $1/\tau$ increases from k_r when $[K^+] = 0$ asymptotically approaching $(k_f + k_r)$ at infinite $[K^+]$. The reverse rate constant for sodium pump cannot be accurately estimated from quench experiments because $k_r \ll k_f$, but the predicted nonzero ordinate ($1/\tau$ axis) intercept has been demonstrated for gastric proton pump (Faller *et al.*, 1991). The maximum value of $1/\tau$ is independent of $[Na^+]$ and is equal to k_f within experimental error. Therefore, fitting $1/\tau$ versus $[K^+]$ data that extend close to the maximum value with eq 2 gives estimates of k_f that do not depend significantly on the values of the other parameters. Two other predictions of Mechanism 1 can be seen by looking at planar cross sections parallel to the $[K^+]$ axis and at right angles to the $[Na^+]$ axis in Figure 1a. First, the predicted titration curve is S-shaped, or sigmoidal. When $[Na^+] = 0$, the K^+ dissociation constant(s) can be estimated without making any assumptions about the number of Na^+ that bind, the affinity of the enzyme for Na^+ , or competitive versus noncompetitive binding of Na^+ and K^+ . The justification for postulating identical and independent sites is that the observed ratio of the minimum of 2 macroscopic K^+ dissociation constants required to describe the sigmoidal shape of the titration curve when $[Na^+] = 0$ is 4 within experimental error (Smirnova & Faller,

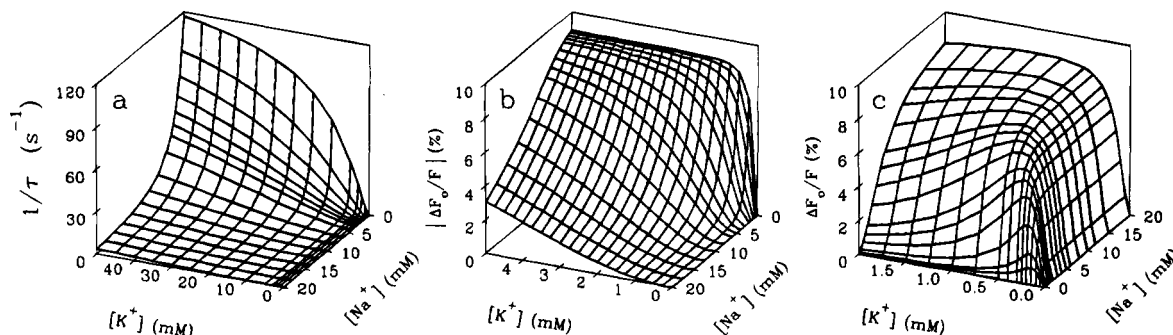


FIGURE 1: Predictions of Mechanism 1, which assumes random binding to two identical and independent sites, for previously estimated parameters at pH 7.4, 15 °C, and $\mu \approx 250$ mM: $k_f = 142$ s⁻¹, $k_r = 0.12$ s⁻¹, and $K_K = 5$ mM (Smirnova & Faller, 1993b) and $K_{Na} = 0.4$ mM (Faller *et al.*, 1994). (a) $1/\tau$ calculated with eq 2. (b) Absolute value of quench amplitude expressed as $\Delta F_o/F$ (%) calculated with eq 6 for $\Delta F_{max}/F = 9\%$. (c) Amplitude of reversal calculated with eq 7.

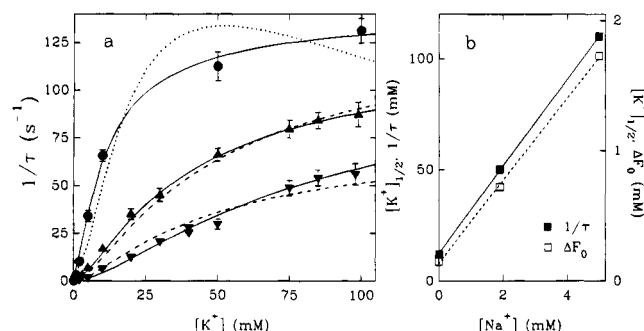


FIGURE 2: Effect of Na⁺ on quench of FITC-modified sodium pump by K⁺. (a) Reciprocal relaxation time is plotted against [K⁺] after mixing at two fixed Na⁺ concentrations. The enzyme syringe contained 150 μ g mL⁻¹ protein, 0.13 mM EDTA, 50 mM Tris-HCl, pH 7.4, at 15 °C, either 1.9 mM (\blacktriangle) or 5 mM (\blacktriangledown) NaCl, and ChoCl to $\mu = 200$ mM from added salt. The reagent syringe contained 50 mM Tris-HCl, the same [NaCl] as the enzyme syringe, KCl at twice the [K⁺] indicated on the concentration axis, and ChoCl to $\mu = 200$ mM from added salt. The 0 mM Na⁺ data (\bullet) are reproduced from Smirnova and Faller (1993b). The lines are fits of eq 2 (solid), eq 12 (dashed), or eq 14 (dots) to the data. The mechanism for which each equation was derived, the constraints imposed on the fit, and the parameter estimates are discussed in the text. (b) Empirical estimates of the half-maximum K⁺ concentrations in plots of $1/\tau$ (\blacksquare) and $\Delta F_o/F$ (\square) versus [K⁺] are plotted against [Na⁺]. The lines are the fits of eq 3 (solid) and eq 8 (dashed) to the data. The values of K_{Na} and K_K estimated from the slopes and intercepts of the least-squares straight lines are reported in the text.

1993b). Second, Na⁺ shifts the inflection point to higher [K⁺]. Equation 3 predicts direct dependence of $[K^+]_{1/2}$ on [Na⁺]. The shape of the curve when K⁺ and Na⁺ are both present depends on the apparent K⁺ dissociation constant.

$$K_K(\text{app}) = K_K \left(1 + \frac{[Na^+]}{K_{Na}} \right) \quad (11)$$

Therefore, to estimate K_K , a value of K_{Na} must be assumed.

The data in Figure 2a confirm the predictions of Mechanism 1. The solid lines are a simultaneous fit of eq 2 to the 1.9 and 5 mM Na⁺ data (triangles) with the constraints $k_r = 0.1$ s⁻¹ and $K_{Na} = 0.4$ mM. The estimated parameter values are $k_f = 126 \pm 3$ s⁻¹ and $K_K = 3.4 \pm 0.1$ mM. To illustrate the direct dependence of $[K^+]_{1/2}$ on [Na⁺], a previously published titration under the same conditions but with [Na⁺] = 0 is reproduced in Figure 2a (circles). Fitting eq 2 to these data with the same constraints gives estimated parameter values $k_f = 142 \pm 1$ s⁻¹ and $K_K = 5.1 \pm 0.3$ mM. In Figure 2b the empirical estimates of $[K^+]_{1/2}$ for $1/\tau$ (filled

squares) are plotted against [Na⁺]. Estimating the microscopic K⁺ and Na⁺ dissociation constants from the slope and ordinate ($1/\tau$ axis) intercept of the least-squares straight line drawn through the data with eq 3 gives $K_K = 5.1 \pm 0.2$ mM and $K_{Na} = 0.63 \pm 0.03$ mM.

Equation 6 also predicts sigmoidal dependence of the quench amplitude on [K⁺], and we have previously demonstrated that amplitudes measured in this type of quench experiment are compatible with the prediction (Smirnova & Faller, 1993b). However, it can be seen from the predicted curves in planes parallel to the [K⁺] axis and perpendicular to the [Na⁺] axis of Figure 1b that the deviation from hyperbolic dependence on [K⁺] occurs when the percentage change in amplitude is too small (<1%) for precise measurements. Therefore, we did not attempt to demonstrate this feature of Mechanism 1, and the amplitudes corresponding to the $1/\tau$ measurements reported in Figure 2a are not shown. However, they confirm the prediction that the maximum observable amplitude change is independent of [Na⁺], decreasing from 0 to $-K_c \Delta F_{max}/(1 + K_c)$ as [Na⁺] is increased (eq 6). Equation 8 predicts linear dependence of $[K^+]_{1/2}$ on [Na⁺]. This prediction is confirmed by the scatter plot of the empirical estimates of $[K^+]_{1/2}$ for ΔF_o (open squares) versus [Na⁺] in Figure 2b. Estimates of K_K and K_{Na} from amplitude data depend on the value of K_c . Approximating k_r by the mean of the values estimated from the two data sets in Figure 2a (134 s⁻¹), constraining $k_r = 0.1$ s⁻¹, and fitting eq 8 to the empirical half-maximum amplitude values in Figure 2b give estimated parameter values $K_K = 4.9 \pm 0.8$ mM and $K_{Na} = 0.43 \pm 0.07$ mM.

Reversal: $1/\tau, \Delta F_o = f([Na^+]_{|K^+})$. In this type of reversal experiment [K⁺] is fixed at some nonzero value and [Na⁺] is chosen as the independent variable. Looking at cross sections of Figure 1c parallel to the [Na⁺] axis and at right angles to the [K⁺] axis, the predicted shape of the amplitude curve changes from apparently hyperbolic to sigmoidal and the inflection point shifts to higher [Na⁺] as [K⁺] is increased. Equation 9 predicts linear dependence of $[Na^+]_{1/2}$ on [K⁺] over most of the concentration range, asymptotically approaching $0.414 K_{Na}$ when [K⁺] = 0. The maximum observable percentage change in fluorescence depends on the fixed [K⁺]. The reason ΔF_o depends on [K⁺] is that the product of the three factors on the right in eq 7 that are independent of [Na⁺] is the amplitude of the quench caused by preincubating with K⁺ (eq 6 with [Na⁺] = 0). Therefore, the maximum fluorescence enhancement observed in a reversal experiment is equal in magnitude to the unobserved fluorescence quench that preceded mixing with Na⁺. Why

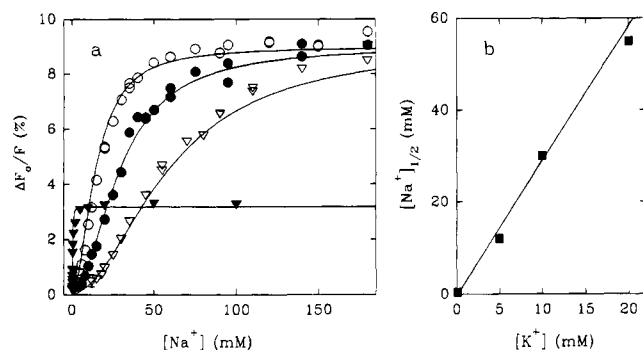


FIGURE 3: Effect of $[K^+]$ used to quench FITC-modified sodium pump on reversal of the conformational change by Na^+ . (a) Percentage change in fluorescence is plotted against $[Na^+]$. The reagent syringe contained 50 mM Tris-HCl, pH 7.4, at 15 °C, twice the $[NaCl]$ shown on the concentration axis, 0.1 mM (\blacktriangledown), 5 mM (\circ), 10 mM (\bullet), or 20 mM (\triangledown) KCl, and ChoCl to $\mu = 200$ mM if $([Na^+] + [K^+]) < 200$ mM. The enzyme syringe contained 150 $\mu\text{g mL}^{-1}$ protein, 0.13 mM EDTA, 50 mM Tris-HCl, the same $[KCl]$ as the titrant syringe, and ChoCl to $\mu = 400$ mM from salt added to both syringes. The solid lines are theoretical curves drawn with eq 7 and the parameter estimates reported in the text. (b) Empirical estimate of the half-maximum $[Na^+]$ for each of the titrations in panel a is plotted against the fixed $[K^+]$ present in the titrations. The solid line was drawn with eq 9 and the same parameter estimates used to calculate the theoretical curves in panel a.

parameters were not estimated from amplitude data can also be understood from eq 7. First, derivation of amplitude equations introduces a fifth parameter (ΔF_{max}), which is not implicit in the proposed mechanism and in practice must be estimated from the experimental data. Second, individual rate constants cannot be estimated from amplitude data, because they occur together in amplitude equations as the ratio K_c . Third, K_c appears in the denominator of eq 7 in combination with K_K and K_{Na} , so that estimates of dissociation constants from amplitude data depend strongly on the ratio of the rate constants.

The data in Figure 3 verify the predictions of eqs 7 and 9. Figure 3a shows that the titration of FITC-enzyme quenched by 0.1 mM K^+ plateaus well below the percentage change in fluorescence to which the titrations of enzyme quenched by higher concentrations of K^+ extrapolate ($\approx 9\%$). It can be seen by expanding the axes that the 0.1 mM K^+ curve is not S-shaped, in contrast to the titrations at higher fixed $[K^+]$ which are clearly sigmoidal. The observation that ΔF_0 becomes sigmoidally dependent on $[Na^+]$ as $[K^+]$ increases is the experimental justification for concluding that more than one Na^+ is involved in reversing the conformational change caused by K^+ . To show that the measured amplitudes in Figure 3a are compatible with the relaxation times in Figure 2a, the theoretical curves were drawn by substituting parameter values that fit the data in Figure 2a ($k_f = 142 \text{ s}^{-1}$, $K_K = 5 \text{ mM}$, $K_{Na} = 0.4 \text{ mM}$, and $k_r = 0.1 \text{ s}^{-1}$) into eq 7 with $\Delta F_{\text{max}}/F = 9\%$. In Figure 3b empirical estimates of the half-maximum Na^+ concentration for the titrations in Figure 3a are plotted against the fixed $[K^+]$. The theoretical line was calculated by substituting the parameter estimates used to draw the curves in Figure 3a into eq 9.

Equation 2 predicts an inverse relationship between $1/\tau$ and $[Na^+]$. The reciprocal relaxation time decreases from $k_f\{[K^+]/([K^+] + K_K)\}^2 + k_r$ when $[Na^+] = 0$, asymptotically approaching k_r at infinite $[Na^+]$. It is possible to demonstrate the expected dependence of $1/\tau$ on $[Na^+]$ in reversal experiments (Faller *et al.*, 1991). However, it can be seen

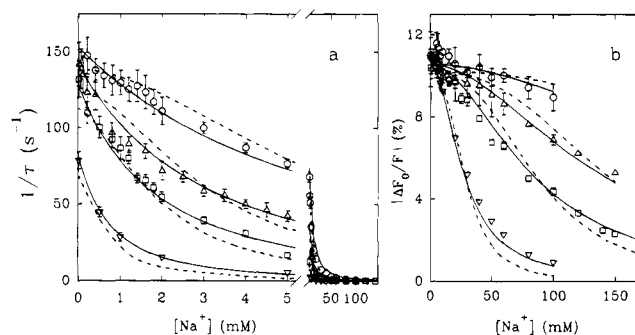


FIGURE 4: Effect of varying $[Na^+]$ on quench of FITC-enzyme by a fixed $[K^+]$. (a) $1/\tau$ measured in final KCl concentrations of 10 mM (∇), 30 mM (\square), 50 mM (Δ), and 100 mM (\circ) KCl is plotted against $[Na^+]$. The reagent syringe contained 50 mM Tris-HCl, pH 7.4, at 15 °C, the $[NaCl]$ shown on the concentration axis, twice the final $[KCl]$, and ChoCl to $\mu = 200$ mM if $([Na^+] + [K^+]) < 200$ mM. The enzyme syringe contained 150 $\mu\text{g mL}^{-1}$ protein, 0.13 mM EDTA, the $[NaCl]$ shown on the concentration axis, and ChoCl to $\mu = 400$ mM from salt added to both syringes. The lines are simultaneous fits of eq 2 (solid) and eq 13 (dashed) to all the data. The corresponding mechanisms, the curve fit constraints, and the parameter estimates are described in the text. (b) Amplitudes observed in the experiments reported in panel a are plotted as percentage change in fluorescence against $[Na^+]$. The solid lines are a simultaneous fit of eq 6 to all the data. The fitting procedure and parameter estimates are given in the text. The dashed lines are a fit of the amplitude equation (not given) for Mechanism 5, described in the text, to all the data.

by comparing cross sections parallel to the $[Na^+]$ axis and at right angles to the $[K^+]$ axis in Figure 1a,c that $1/\tau$ increases sharply while ΔF_0 decays to zero as $[Na^+]$ is reduced, so that only part of the total change in $1/\tau$ can be measured precisely. For example, less than 6% of the predicted change in $1/\tau$ with $[Na^+]$ can be observed experimentally when $[K^+] \geq 5 \text{ mM}$. Therefore, no attempt was made to estimate K_{Na} , which depends on the shape of the curve, by fitting eq 2 to this type of experiment, and the reciprocal relaxation times corresponding to the amplitudes in Figure 3a are not shown. On the other hand, the amplitude increases as $[Na^+]$ increases, and $1/\tau$ asymptotically approaches k_r . An estimate of k_r that is essentially independent of the other parameters can be obtained from the minimum value approached in plots of $1/\tau$ for the reversal reaction versus $[Na^+]$. We estimated $1/\tau = 0.105 \pm 0.006 \text{ s}^{-1}$ ($n = 21$, $0.1 \leq [K^+] \leq 20 \text{ mM}$) from the measurements that scattered about a minimum value and imposed the constraint $k_r = 0.1 \text{ s}^{-1}$ to reduce the number of estimated parameters in fits of data from other types of experiments.

Quench: $1/\tau, \Delta F_0 = f([Na^+])_{[K^+]}$. The amplitude of a quench experiment increases as $[Na^+]$ decreases (Figure 1b). Therefore, the experimental limitation of the reversal experiment described in the preceding paragraph can be circumvented by choosing Na^+ as the independent variable in quench experiments. Figure 4 shows that the functional dependence of $1/\tau$ and ΔF_0 on $[Na^+]$ can be measured over the entire concentration range. Data from quench experiments as a function of $[Na^+]$ was used to test the prediction of mechanism 1 that the ratio of the macroscopic Na^+ dissociation constants (K_{Na2}/K_{Na1}) is 4.

In Figure 4a, $1/\tau$ is plotted against $[Na^+]$. The concentration axis is broken to show the region in which $1/\tau$ changes rapidly with $[Na^+]$ more clearly. At least second-order terms in $[Na^+]$ are needed to fit the reciprocal relaxation times in Figure 4a (not shown). Although the Na^+ and K^+ dissociation constants occur together in the relaxation expression (eq

2) as apparent dissociation constant(s) (eq 11), estimate(s) of K_{Na} that are quasi-independent of K^+ binding can be obtained from quench experiments as a function of $[Na^+]$ by assuming that K_K is known from quench experiments as a function of $[K^+]$ with $[Na^+] = 0$. The prediction that $K_{Na2}/K_{Na1} = 4$ was tested by rewriting eq 2 in terms of macroscopic Na^+ dissociation constants with the help of eq 10 and globally fitting the resulting expression to the data in Figure 4a with the constraints $k_r = 0.1 \text{ s}^{-1}$ and $K_K = 5 \text{ mM}$, the value of K_K estimated from the $[Na^+] = 0$ data in Figure 2a. The estimated forward rate constant is $k_f = 167 \pm 1.5 \text{ s}^{-1}$, and the estimated macroscopic Na^+ dissociation constants are $K_{Na2} = 1.28 \pm 0.10 \text{ mM}$ and $K_{Na1} = 0.26 \pm 0.02 \text{ mM}$, so that the ratio $K_{Na2}/K_{Na1} = 4.9 \pm 0.8$ is 4 within experimental error. The solid theoretical lines in Figure 4a were drawn with the parameters estimated by fitting eq 2 to the data $k_f = 166 \pm 2 \text{ s}^{-1}$, $K_K = 4.4 \pm 0.3 \text{ mM}$, and $K_{Na} = 0.47 \pm 0.03 \text{ mM}$ with the constraint $k_r = 0.1 \text{ s}^{-1}$. A plot of the empirical half-maximum Na^+ concentration versus $[K^+]$ (not shown) is linear as predicted by eq 4, and the estimates of K_{Na} and K_K from the slope and ordinate intercept are in reasonable agreement with the values obtained by fitting eq 2 to all of the experimental points.

Figure 4b is a plot of the amplitudes corresponding to the $1/\tau$ measurements in Figure 4a against $[Na^+]$. It can be seen from cross sections of Figure 1b parallel to the $[Na^+]$ axis and perpendicular to the $[K^+]$ axis that the dependence of $\Delta F_o/F$ on $[Na^+]$ becomes sigmoidal and the inflection point shifts to higher $[Na^+]$ as $[K^+]$ is increased. Preincubating the enzyme with increasing $[Na^+]$ before mixing with a fixed $[K^+]$ inverts the S-shape observed in reversal experiments as a function of $[Na^+]$ (Figure 3a), because ΔF_o is oppositely related to $[Na^+]$ in the quench amplitude (inversely) and reversal amplitude (directly) equations (eqs 6 and 7, respectively). The data in Figure 4b confirm these predictions. The solid lines are a simultaneous fit of eq 6 to all of the data that gives estimated parameter values $K_{Na} = 0.30 \pm 0.01 \text{ mM}$ and $\Delta F_{max}/F = 10.6 \pm 0.1\%$, subject to the constraints $k_r = 0.1 \text{ s}^{-1}$, $k_f = 166 \text{ s}^{-1}$, and $K_K = 4.4 \text{ mM}$ obtained from $1/\tau$ data. The estimates of K_{Na} obtained from the equilibrium data in Figure 4b and the kinetic data in Figure 4a were averaged to obtain the estimate of $K_{Na} = 0.38 \pm 0.04 \text{ mM}$ (0.4 mM) imposed as a constraint in fitting other types of experiments. The half-maximum $[Na^+]$ at the three lower K^+ concentrations can be estimated empirically and is linearly related to $[K^+]$ as predicted by eq 9 (not shown).

Reversal: $\Delta F_o = f([K^+])_{[Na^+]}$. If a fixed $[Na^+]$ is used to reverse the quench of FITC-modified Na,K-ATPase fluorescence by varying concentrations of K^+ , Mechanism 1 predicts a peak in the titration curve. A cross section parallel to the $[K^+]$ axis and perpendicular to the $[Na^+]$ axis in Figure 1c illustrates this prediction. The reason the titration curve passes through a maximum can be understood by looking at eq 7 for the case $[Na^+] = 0$. There is a factor that depends only on $[K^+]$ and determines the magnitude of the quench, as well as a factor containing both $[Na^+]$ and $[K^+]$ that determines the extent of the reversal as a function of $[Na^+]$. When $[K^+] = 0$ there is no reversal because the choice of buffer and μ shifts the equilibrium between conformations far toward E_1 . Initially, preincubating the enzyme with increasing $[K^+]$ increases the reversal amplitude because the factor that determines the magnitude of the quench dominates, that is, increasing $[K^+]$ in the preincubation converts

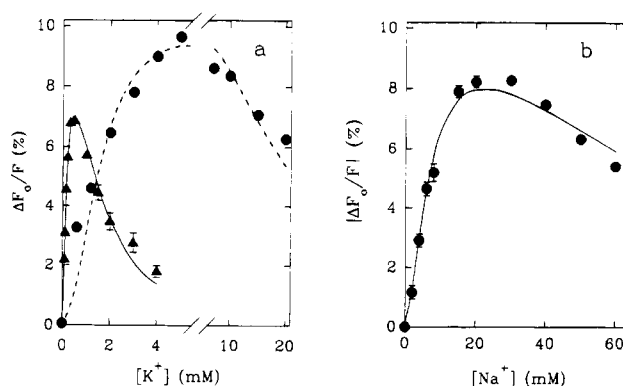


FIGURE 5: Peak in amplitude titrations. (a) Reversal of conformational change in FITC-enzyme quenched with varying amounts of K^+ by a fixed, final $[Na^+]$. The percentage change in fluorescence is plotted. In the experiment denoted by triangles, the enzyme syringe contained $150 \mu\text{g mL}^{-1}$ protein, 0.13 mM EDTA, 50 mM Tris-HCl, pH 7.4, at 15°C , the $[KCl]$ shown on the concentration axis, and ChoCl to $\mu = 200 \text{ mM}$ from added salt. The reagent syringe contained 50 mM Tris-HCl, the same $[KCl]$ as the enzyme syringe, 10 mM NaCl ($[Na^+]_{\text{final}} = 5 \text{ mM}$), and ChoCl to $\mu = 200 \text{ mM}$ from added salt. The solid line is a curve fit of eq 7 to the data with the constraints reported in the text. In the experiment indicated by circles, the enzyme syringe contained $150 \mu\text{g mL}^{-1}$ protein, 0.13 mM EDTA, 50 mM Tris-HCl, 5 mM NaCl ($[NaCl]_{\text{initial}}$), the $[KCl]$ shown on the concentration axis, and ChoCl to $\mu = 200 \text{ mM}$ from added salt. The reagent syringe contained 50 mM Tris-HCl, the same $[KCl]$ as the enzyme syringe, 125 mM NaCl ($[NaCl]_{\text{final}} = 65 \text{ mM}$), and ChoCl to $\mu = 200 \text{ mM}$ from added salt. The dashed line is a curve fit of eq 5 to the data with the constraints described in the text. (b) Quench of FITC-enzyme preincubated in 1.8 mM KCl and varying concentrations of Na^+ by a fixed, final $[K^+] = 21.8 \text{ mM}$. The absolute value of the percentage change in fluorescence is plotted. The enzyme syringe contained $150 \mu\text{g mL}^{-1}$ protein, 50 mM Tris-HCl, 0.13 mM EDTA, the $[NaCl]$ shown on the abscissa, 1.8 mM KCl, and ChoCl to $\mu = 200 \text{ mM}$ from added salt. The reagent syringe contained 50 mM Tris-HCl, the same $[NaCl]$ as the enzyme syringe, 41.8 mM KCl, and ChoCl to $\mu = 200 \text{ mM}$ from added salt. The line is a fit of eq 5 to the data. The curve fit constraints and parameter estimates are given in the text.

more enzyme to E_2 , which is converted back to E_1 by mixing with $[Na^+]$. As $[K^+]$ is increased farther, the factor that determines the extent of the reversal becomes dominant. The reversal amplitude passes through a maximum and decreases as $[K^+]$ increases, because the fixed $[Na^+]$ used to reverse the conformational change is not high enough to displace K^+ from the binding sites on the E_1 conformation and completely reverse the fluorescence quench.

Figure 5a confirms the prediction of Mechanism 1. In the experiment represented by triangles, the initial $[Na^+]$ was zero. The solid line is a curve fit of eq 7 to the data with the constraints $k_f = 142 \text{ s}^{-1}$, $K_{Na} = 0.4 \text{ mM}$, and $k_r = 0.1 \text{ s}^{-1}$ that gives parameter estimates $K_K = 4.8 \pm 0.3 \text{ mM}$ and $\Delta F_{max}/F = 8.25 \pm 0.4\%$. The titration denoted by circles shows that mechanism 1 also explains the more general case when $[Na^+]_{\text{initial}} \neq 0$. The dashed line is a curve fit of eq 5 to the data with the same constraints that gives estimated parameter values $K_K = 4.4 \pm 0.2$ and $\Delta F_{max}/F = 11.2 \pm 1.0\%$.

Quench: $\Delta F_o = f([Na^+])_{[K^+]_{\text{initial}} \neq 0}$. Conversely, a peak in the titration curve obtained by quenching FITC-enzyme with a fixed $[K^+]$ is predicted, if $[K^+]_{\text{initial}} \neq 0$ and Na^+ is the independent variable. In practice, observing a curve that goes through a maximum is a rigorous test of the proposed mechanism, because correct estimates of both the ion affinities and the mathematical relationship coupling ion binding to the conformational change are required to

design the experiment. The initial and final K^+ concentrations to use in the experiment were predicted by generating theoretical curves with eq 5.

Figure 5b shows experimental confirmation that there is a peak in a plot of amplitude versus $[Na^+]$ for appropriate choices of $[K^+]_{\text{initial}} = 1.8 \text{ mM}$ and $[K^+]_{\text{final}} = 21.8 \text{ mM}$ in a quench experiment. The quench amplitude is zero when $[Na^+] = 0$, because $[K^+]_{\text{initial}}$ was chosen so that all of the enzyme started out in the E_2 conformation. The quench amplitude initially increases as enzyme is preincubated in higher Na^+ concentrations, because Na^+ converts an increasing fraction of the enzyme to the E_1 conformation with higher fluorescence intensity and $[K^+]_{\text{final}}$ is high enough to completely convert the enzyme back to the E_2 conformation. The amplitude passes through a maximum and decreases when $[K^+]_{\text{final}}$ is no longer high enough to compete with Na^+ and completely quench the Na^+ reversal of the quench caused by $[K^+]_{\text{initial}}$. The solid line is a curve fit of eq 5 to the data with the constraints $k_f = 166 \text{ s}^{-1}$, $K_K = 5 \text{ mM}$, and $k_r = 0.1 \text{ s}^{-1}$ that gives estimated parameter values $K_{Na} = 0.5 \pm 0.4 \text{ mM}$ and $\Delta F_{\text{max}}/F = -9.6 \pm 0.2\%$.

DISCUSSION

The new idea in this paper is that the conformational change reported by FITC modification of sodium pump may be controlled by random binding of the transported ions to identical and independent sites. The experimental basis for proposing an equivalent site mechanism is that the ratio of the macroscopic dissociation constants estimated from sigmoidal plots of $1/\tau$ for the conformational change as a function of $[K^+]$ when $[Na^+] = 0$ is 4 within experimental error (Smirnova & Faller, 1993b), independent of both the enzyme preparation and the intensive variable temperature (Faller *et al.*, 1994). Four is the numerical ratio expected for statistical binding to two equivalent sites that do not interact (Edsall & Wyman, 1958). A ratio near 4 has been independently measured at lower ionic strength by Grell and co-workers (Doludda *et al.*, 1994), who report $K_{K_1} = 0.2 \text{ mM}$ and $K_{K_2} = 0.7 \text{ mM}$ without quoting the uncertainty in their estimates.

Evidence that More than One Na^+ Binds. In Mechanism 1 the conformational change caused by K^+ begins to reverse as soon as a single Na^+ binds because Na^+ binding is coupled to the protein rearrangement. However, $[Na^+]^2$ terms are required to explain sigmoidal dependence of the reversal amplitude on $[Na^+]$. Therefore, at least two Na^+ must bind to explain the data in Figure 3a at the higher K^+ concentrations. Mechanism 1 assumes that Na^+ and K^+ bind competitively to two identical and independent sites, so predictions of the proposed mechanism that can be tested experimentally are, first, Na^+ competes with K^+ at both sites and, second, the ratio of the macroscopic Na^+ dissociation constants equals 4.

Evidence Na^+ and K^+ Bind Competitively. Karlsh (1980) proposed that Na^+ reverses the K^+ quench of FITC-enzyme by competitively binding at a single site on the E_1 conformation, because the apparent dissociation constant for K^+ in equilibrium titrations depended linearly on $[Na^+]$ (eq 11). However, linear dependence of $[K^+]_{1/2}$ on $[Na^+]$ is not predicted for competitive binding of Na^+ to the two sites necessary to explain sigmoidal dependence of $1/\tau$ on $[K^+]$, except in the special case where binding of Na^+ to two sites

can be described by a single intrinsic dissociation constant. Moreover, equilibrium titrations may be misleading (Lin & Faller, 1993) because of heterogeneous labeling of sodium pump by FITC (Xu, 1989).

To obtain unequivocal evidence for competitive binding and show that K^+ and Na^+ compete at both of the sites required to explain sigmoidal titration curves, we derived the relaxation expression for Mechanism 2 in which non-competitive binding of Na^+ and K^+ is assumed.

$$\frac{1}{\tau} = K_f \left[\frac{[K^+]}{([K^+] + K_K) \left(1 + \frac{[Na^+]}{K_{Na}} \right)} \right]^2 + k_r \quad (12)$$

In contrast to eq 2 for competitive binding, eq 12 predicts dramatic dependence of the maximum $1/\tau$ on $[Na^+]$, extrapolating to $k_f/(1 + [Na^+]/K_{Na})^2 + k_r$ at infinite $[K^+]$. We have previously shown that titrations beginning above the inflection point in plots of $1/\tau$ versus $[K^+]$ cannot be fit by eq 12 when Na^+ is also varied (Faller *et al.*, 1994). The dashed lines in Figure 2a show a simultaneous fit of eq 12 with no constraints to the data collected in the presence of Na^+ . It is qualitatively clear from comparing the solid and dashed lines through the triangular points in Figure 2a that eq 2 also fits data below the inflection point better than eq 12. Quantitative measures of the poorer fit of Mechanism 2 compared with Mechanism 1 are more than a doubling of the root-mean-square deviation (rmsd) from 1.5 s^{-1} (eq 2) to 3.8 s^{-1} (eq 12) and a decrease in the number of runs from 9 (eq 2) to 4 (eq 12). Runs are arrangements of residuals into groups with a + or - sign, and an increased number of runs indicates more random scatter of the data points about the theoretical line (Draper & Smith, 1981). The competitive binding mechanism also fits the $1/\tau$ as a function of $[Na^+]$ data in Figure 4a better than the noncompetitive binding model (not shown). In this case, rmsd nearly triples from 3.4 s^{-1} (eq 2) to 9.0 s^{-1} (eq 12), and the number of runs decreases from 17 (eq 2) to 11 (eq 12).

The somewhat lower estimates of K_K obtained by fitting the titrations in Figure 2a (3.4 mM) and Figure 4a (4.7 mM) with Na^+ present, compared to the value (5.1 mM) estimated from the titration in Figure 2a with $[Na^+] = 0$, may be real. The reason is that there is evidence Cho^+ and $Tris^+$ compete with K^+ when Na^+ is absent (Lin & Faller, 1993). The Cho^+ dissociation constant (K_{Cho}) can be roughly estimated as $>250 \text{ mM}$ from the cited values of $K_K \pm Na^+$ and the minimum $[ChoCl]$ at any $[K^+]$ in the titration. It would be technically difficult to quantify the effect of Cho^+ any better, and introducing Cho^+ into Mechanism 1 would complicate the expressions for $1/\tau$ and ΔF_0 . The important points are, first, that any effect of Cho^+ and $Tris^+$ on parameter estimates is small, and, second, that Cho^+ and $Tris^+$ do not affect the ratio of macroscopic dissociation constants for K^+ or Na^+ at all, because the factors containing $[ChoCl]$, $[Tris]$, K_{Cho} , and K_{Tris} cancel when equations for apparent constants (cf. eq 11) are divided to obtain the ratio of macroscopic constants.

Evidence for Hybrid Enzyme Species with Both Na^+ and K^+ Bound. It is not necessary to assume that Na^+ and K^+ bind simultaneously to explain the sigmoidal dependence of either $1/\tau$ on $[K^+]$ in a quench experiment or ΔF_0 on $[Na^+]$ in a reversal experiment. However eq 13, the relaxation expression for Mechanism 3 in which metal hybrids are not

Table 1: Comparison of Equivalent Site Mechanisms

			mechanism							
variable		data in figure	1: $\text{KE}_1\text{K} \rightarrow \text{KE}_2\text{K}$		5: $\text{E}_1\text{K}_3 \rightarrow \text{E}_2\text{K}_3$		6: $\text{E}_1\text{K}_2 \rightarrow \text{E}_2\text{K}_2$ $\text{E}_1\text{K}_3 \rightarrow \text{E}_2\text{K}_3$		7: ^a $\text{E}_1\text{K}_2 \rightarrow \text{E}_2\text{K}_2$ $\text{E}_1\text{K}_3 \rightleftharpoons \text{E}_2\text{K}_3$	
dependent	independent		rmsd ^b	runs ^c	rmsd	runs	rmsd	runs	rmsd	runs
$1/\tau$	$[\text{K}^+]$	2a (●)	1.884	6	2.010	5	3.216	3	1.967	6
$1/\tau$	$[\text{Na}^+]$	4a	3.502	14	3.282	17	3.564	19	3.122	14
$\Delta F_o/F$	$[\text{Na}^+]$	4b	0.383	12	0.664	8	0.576	11	0.551	10
$1/\tau$	$[\text{K}^+]$	2a (▲, ▼)	1.745	7	2.632	4	1.589	7	1.556	10
$\Delta F_o/F$	$[\text{Na}^+]$	3a	0.302	20	0.405	10	0.446	10	0.325	7
$\Delta F_o/F$	$[\text{K}^+]$	5a (▲)	0.292	5	0.522	4	0.817	3	0.566	3
$\Delta F_o/F$	$[\text{K}^+]$	5a (●)	0.788	5	1.228	5	0.513	5	0.711	5
$\Delta F_o/F$	$[\text{Na}^+]$	5b	0.318	5	0.334	5	0.579	4	0.220	5

^a The double arrow indicates a different k_f for E_1K_3 than for E_1K_2 . ^b The rmsd units are s^{-1} when the independent variable is $1/\tau$ and % when the independent variable is ΔF_o . ^c Number.

allowed to form,

$$\frac{1}{\tau} = k_f \left[\frac{[\text{K}^+]^2}{[\text{K}^+]^2 + 2K_K[\text{K}^+] + K_K^2 \left(1 + \frac{[\text{Na}^+]^2}{K_{\text{Na}}} \right)} \right] + k_r \quad (13)$$

predicts a different dependence than eq 2 predicts of $1/\tau$ on $[\text{Na}^+]$ for quench experiments in which Na^+ is chosen as the independent variable. The dashed lines in Figure 4a show that eq 13 predicts convex curvature beginning at the origin of $1/\tau$ versus $[\text{Na}^+]$ plots that is not observed experimentally. Therefore, the possibility that hybrid enzyme species, with both Na^+ and K^+ bound, are not formed is excluded by the data.

Evidence that Na^+ Binds to Two Equivalent Sites. In a preliminary communication, we showed that reversal experiments as a function of $[\text{Na}^+]$ at one $[\text{K}^+]$ could be explained by competitive binding to two sites with the constraint that $K_{\text{Na}_2}/K_{\text{Na}_1} = 4$ (Faller *et al.*, 1994). In addition to showing that at least two Na^+ must bind to explain the reversal reaction, Figure 3a strengthens the evidence for a $K_{\text{Na}_2}/K_{\text{Na}_1}$ ratio of 4 by demonstrating that a family of amplitude titration curves with different shapes can be satisfactorily fit by eq 7. Still stronger evidence that Na^+ binds to identical and independent sites is provided by the experiment in Figure 4a. Estimates of K_{Na_1} and K_{Na_2} that are quasi-independent of assumptions about K^+ binding were obtained by fitting eq 2, written in terms of macroscopic Na^+ dissociation constants, to the data with K_K constrained to the value estimated from experiments with $[\text{Na}^+] = 0$. The estimated ratio $K_{\text{Na}_2}/K_{\text{Na}_1} = 4.9 \pm 0.8$ is 4 within experimental error.

Equivalent Binding of Na^+ and K^+ to Three Sites. Since the consensus stoichiometry of Na^+ transport is 3, and it is easiest to conceptualize competitive binding to equal numbers of sites, we have derived algebraic equations for mechanisms in which the transported ions competitively bind to three identical, noninteracting sites. The three possibilities that would account for sigmoidal dependence of $1/\tau$ on $[\text{K}^+]$ are Mechanism 4 which assumes only E_1K_2 changes conformation, Mechanism 5 which assumes only E_1K_3 changes conformation, or Mechanism 6 which assumes both E_1K_2 and E_1K_3 change conformation. The first possibility can be rejected, because it also predicts a peak in $1/\tau$ versus $[\text{K}^+]$ curves that is not observed experimentally. Equation 14 is the relaxation expression for Mechanism 4.

$$\frac{1}{\tau} = k_f \left\{ [\text{K}^+]^2 \left[\frac{[\text{K}^+]^3}{3K_K} + \left(1 + \frac{[\text{Na}^+]}{K_{\text{Na}}} \right) [\text{K}^+]^2 + K_K \left(1 + \frac{[\text{Na}^+]}{K_{\text{Na}}} \right)^2 [\text{K}^+] + \frac{K_K^2}{3} \left(1 + \frac{[\text{Na}^+]}{K_{\text{Na}}} \right)^3 \right] \right\} + k_r \quad (14)$$

Equation 14 was simultaneously fit to all of the data in Figure 2a. However, only the $[\text{Na}^+] = 0$ curve fit is shown by a dotted line to avoid overcrowding the figure. The reciprocal relaxation time increases sigmoidally as the two K^+ required for the conformational change bind, reaches a maximum, and then decreases as the inhibitory third K^+ site fills. Equation 15 is the relaxation expression for Mechanism 5.

$$\frac{1}{\tau} = k_f \left[\frac{[\text{K}^+]}{[\text{K}^+] + K_K \left(1 + \frac{[\text{Na}^+]}{K_{\text{Na}}} \right)} \right]^3 + k_r \quad (15)$$

The expressions in square brackets in eqs 14 and 15 are the fractions of the enzyme in the E_1 conformation with two ($\chi_{\text{E}_1\text{K}_2}$) and three ($\chi_{\text{E}_1\text{K}_3}$) K^+ bound, respectively. Equation 16 is the relaxation expression for Mechanism 6.

$$\frac{1}{\tau} = k_f (\chi_{\text{E}_1\text{K}_2} + \chi_{\text{E}_1\text{K}_3}) + k_r \quad (16)$$

Mechanism 7 is an elaboration of Mechanism 6 in which different forward rate constants for the E_1K_2 ($k_{f_{\text{E}_1\text{K}_2}}$) and E_1K_3 ($k_{f_{\text{E}_1\text{K}_3}}$) species are considered. Amplitude equations were also derived for each of these mechanisms but are not given for the sake of brevity.

In Table 1, two quantitative measures of "goodness of fit" for each of the equivalent site mechanisms that correctly predict the shapes of the experimental curves are compared. The same strategy for estimating parameters and fitting data with the equations derived for Mechanism 1 was used to analyze Mechanisms 5–7. Lower rmsd and greater number of runs indicate a better fit. The dashed lines in Figure 4b illustrate what approximately doubling rmsd and halving the number of runs means by showing the fit of the quench amplitude equation for Mechanism 5 to the data.

Mechanism 1 gives the "best" fit to four data sets [Figures 2a (●), 4b, 3a, and 5a (▲)]. Mechanism 1 also gives the most consistent parameter estimates and values for which there is precedent in the literature. The means and standard deviations in the parameter estimates obtained by fitting Mechanism 1 to the data in this paper and previously published experiments under the same experimental condi-

tions are $k_f = 150 \pm 19 \text{ s}^{-1}$ ($N = 4$), $k_r = 0.13 \pm 0.03 \text{ s}^{-1}$ ($N = 3$), $K_K = 4.8 \pm 1.2 \text{ mM}$ ($N = 4$), and $K_{Na} = 0.38 \pm 0.12 \text{ mM}$ ($N = 2$), where N indicates the number of independent data sets. Direct measurements of Na^+ and K^+ binding to porcine enzyme give apparent dissociation constants of about 0.2 mM for both ions (Yamaguchi & Tonomura, 1979). Since the cited binding measurements were made in 75 mM ChoCl and 15 mM imidazole-HCl, the value 0.2 mM is for dissociation from the E_1 conformation of the enzyme and can be compared directly with our estimate of $K_{Na} = 0.38 \text{ mM}$. The value 0.2 mM from direct binding measurements for K^+ dissociation must be compared to $[\text{K}^+]_{1/2}$, because K^+ binding is coupled to the conformational change. Substituting the mean kinetic estimates of k_f , k_r , and K_K into eq 8 gives $[\text{K}^+]_{1/2} = 0.15 \text{ mM}$ for $[\text{Na}^+] = 0$, in good agreement with the direct binding estimate.

Mechanism 5 does not fit the data in any data set best and in addition predicts a different transport stoichiometry for K^+ (3) than the stoichiometry (2) usually observed in transport, occlusion, and direct binding studies. Mechanism 6 fits one data set [Figure 5a (●)] best, and Mechanism 7 fits three data sets [Figures 4a, 2a (▲, ▼), and 5b] best. These mechanisms demonstrate that the conformational change reported by FITC modification is not incompatible with stoichiometric measurements indicating that three Na^+ bind and are transported. However, since neither Mechanism 6 nor 7 fit the kinetic data better than Mechanism 1, this study does not strengthen the evidence from transport, binding, and occlusion experiments for three Na^+ sites.

Uniqueness of Mechanism. The improved fit of Mechanism 7, which assumes two forward rate constants and therefore contains an additional parameter, over Mechanism 6 illustrates the inherent limitation of kinetic studies. Although Mechanism 1 satisfactorily explains the kinetic data, more complicated mechanisms cannot be ruled out. The data could obviously be explained by ordered and anticooperative binding to two sites coincidentally differing in their affinity for both K^+ and Na^+ by a factor of 4. The minimum number of parameters in an anticooperative binding scheme is six (two rate constants and four dissociation constants) and increases rapidly if the order of binding to hybrid forms is considered or three binding sites are assumed. We did not derive algebraic equations and test anticooperative binding mechanisms, because the fit of mechanism 1 to the data is already well within the precision with which we can measure the rate and magnitude of the conformational change reported by FITC modification of sodium pump with stopped-flow fluorometry.

Equations that assume binding to identical and independent sites have been used to fit both active and passive transport data by several laboratories (Garay & Garrahan, 1973; Karlsh & Stein, 1985; Sachs, 1986). The remarkable agreement between the constants deduced from transport studies for Na^+ and K^+ dissociation from internal sites and the dissociation constants from E_1 estimated from kinetic studies of the conformational change in FITC-enzyme is evidence that fluorescein on lysine 501 reports a step in the transport mechanism (Faller *et al.*, 1991). Therefore, transport studies support an equivalent site interpretation of the conformational change in unphosphorylated sodium pump, with the caveat that not enough data have been collected below the inflection point in transport experiments to obtain quantitative evidence for identity of the ion binding sites (Sachs, 1967). The conformational change reported by

FITC modification is the only reaction for which precise enough data has been obtained to conclude that the ratio of the dissociation constants for both K^+ and Na^+ is experimentally indistinguishable from 4 and therefore suggestive of binding to identical and independent sites.

Generality of Mechanism. There is conflicting evidence on whether interaction of K^+ and its congeners with the E_2 conformation of sodium pump is consistent with binding to identical and independent sites. On the one hand, equations that assume equivalent binding fit data for K^+ influx into red blood cells (Sachs & Welt, 1967). On the other hand, two laboratories have published evidence for ordered release of Rb^+ from the occluded state of Na,K-ATPase but only from phosphoenzyme formed from inorganic phosphate which is presumed to be in the E_2 conformation (Glynn *et al.*, 1985; Forbush, 1987). When deocclusion is brought about by ATP, which accelerates the $E_2 \rightarrow E_1$ transition and is followed by release of the ions from E_1 , the two Rb^+ sites are experimentally indistinguishable (Forbush, 1987). An interesting possibility is that phosphorylation introduces asymmetry into the molecule.

There is no discrepancy between the "concentration dependence of equilibrium occlusion" and the "sigmoidal dependence of the rate of transition from E_1 to E_2 with FITC-modified Na,K-ATPase " (Esmann, 1994), because the inflection point in amplitude curves predicted by eq 6 is difficult to observe experimentally, even when $\mu = 250 \text{ mM}$ and $[\text{Na}^+] \neq 0$ (Figure 1b). Hyperbolic occlusion curves are observed at lower μ , where K^+ congeners appear to bind tighter, and in the absence of Na^+ without keeping μ constant (Shani *et al.*, 1987).

It is tempting to cite sigmoidal effects of Na^+ and K^+ on the conformational change reported by eosin (Skou & Esmann, 1983) as support for the equivalent site mechanism proposed here to explain the conformational change in FITC-modified Na,K-ATPase . Mechanism 1 provides a simpler explanation of many of the observations made with eosin. For example, eq 2 predicts an increase in the observed rate constant for the E_2 to E_1 conformational change with increasing $[\text{K}^+]$ without introducing a low-affinity K^+ site on E_2 that accelerates the reaction (Skou & Esmann, 1983; Esmann & Skou, 1983). However, the $[\text{Na}^+]$ dependence of the observed first-order rate constant for the reverse reaction ($E_2 \rightarrow E_1$) reported by eosin (Skou & Esmann, 1983; Esmann, 1994) is in the opposite direction to the prediction of eq 2, that is, directly instead of inversely proportional to $[\text{Na}^+]$. Therefore, either FITC labeling and eosin binding report different conformational changes or a systematic error is being made in experiments with one of the reporter molecules. Ionic strength was not controlled in the experiments with eosin. However, in two experiments in which the μ jump was constant, because lower $[\text{Na}^+]$ was compensated by ChoCl , the rate constant for the E_2 to E_1 conformational change either did not change or was inversely related to $[\text{Na}^+]$ as predicted by eq 2 and demonstrated for reversal of the FITC reaction (Faller *et al.*, 1991). Study of the $E_1 \rightarrow E_2$ transition with eosin is complicated by an eosin off-rate that is not diffusion controlled, but the observed first-order rate constant does appear to increase with $[\text{K}^+]$ as predicted by eq 2 (Skou & Esmann, 1983). Therefore, it seems likely that the conformational change reported by eosin can also be satisfactorily explained by Mechanism 1, if all of the experimental variables are carefully controlled, and that both extrinsic fluorophores are reporting the same conformational change.

In a series of recent articles, Grell and co-workers have suggested that the high-intensity fluorescent state reported by FITC modification of sodium pump is not E_1 (Grell *et al.*, 1991, 1992, 1994). The conclusion that fluorescein reports a change from E_2 to a conformation (F_1) different from E_1 is based on two observations. First, the Na^+ dissociation constant estimated from equilibrium titrations is larger than estimates of K_{Na} from direct binding measurements, and second, approximately the same numerical dissociation constant is estimated from equilibrium titrations for Na^+ , Cho^+ , and a number of other monovalent cations. The first observation is predicted by Mechanism 1. The midpoint of an equilibrium titration with Na^+ is $[\text{Na}^+]_{1/2}$ not K_{Na} (eq 9), because Na^+ binding is reported indirectly by the fluorescence change resulting from the conformational change. The theoretical line in Figure 3b demonstrates that the $[\text{Na}^+]_{1/2}$ values observed in Figure 3a can be calculated with eq 9. Both nonselective and selective binding contribute to the second observation of Grell and co-workers. Since μ varied in their titrations, part of the fluorescence change measured by Grell *et al.* is an ionic strength effect (Lin & Faller, 1993) that is expected to give the dissociation constant for nonspecific ion pair formation by any monovalent cation. The other contributor to the fluorescence change observed by Grell and co-workers is the conformational change between E_1 and E_2 . We have demonstrated that Cho^+ , as well as Na^+ , causes a slow change in the fluorescence of fluorescein at the antibody-inaccessible, ATP-protectable site that reports the change between E_2 and E_1 conformations (Abbott *et al.*, 1991) by stopped-flow measurements that temporally resolve the signals from specific and nonspecific binding (Faller *et al.*, 1994). Mechanism 1 predicts that the half-maximum titrant concentration for this fraction of the fluorescence change will be larger than the titrant's true dissociation constant because of competition with histidine, which is responsible for the enzyme starting out in the E_2 conformation (Lin & Faller, 1993). Broadened titration curves that were interpreted as evidence for two Na^+ affinities (Grell *et al.*, 1991) support the conclusion that the fluorescence change measured in histidine buffer when μ changes reports more than one reaction.

More recently an increase in $1/\tau$ with $[\text{ChoCl}]$ has been interpreted as kinetic evidence that fluorescein reports a change from E_2 to a new conformation (F_1) (Doludda *et al.*, 1994). However, since μ must have changed when the reactants were mixed in these stopped-flow experiments by Grell and co-workers, an alternative interpretation of their data is that an increase in $1/\tau$ was observed because k_t increases 1 order of magnitude between $\mu = 20$ mM and $\mu = 250$ mM (unpublished data). The data points in Figure 4a show clearly that $1/\tau$ depends inversely on $[\text{Na}^+]$, if stopped-flow experiments are designed so that there is negligible change in μ when FITC-labeled enzyme and monovalent cation are mixed, and the solid theoretical lines show that the experimental observations can be satisfactorily fit by eq 2. Mechanism 1 explains the reaction reported by FITC modification of Na,K-ATPase with the two major conformations of the pump that have been implicated in ion transport.

ACKNOWLEDGMENT

The authors are indebted to Martin Stengelin and Vladimir Kasho for their contributions to the derivations of several equations.

REFERENCES

- Abbott, A. J., Amler, E., & Ball, W. J., Jr. (1991) *Biochemistry* 30, 1692–1701.
- Changeux, J.-P. (1990) *Trends Pharmacol. Sci.* 11, 485–492.
- Doludda, M., Lewitzki, E., Ruf, H., & Grell, E. (1994) in *The Sodium Pump: Structure, Mechanism, Hormonal Control and its Role in Disease* (Bamberg, E., & Schoner, W., Eds.) pp 629–632, Steinkopff, Darmstadt.
- Draper, N. R., & Smith, H. (1981) *Applied Regression Analysis*, pp 157–162, John Wiley & Sons, New York.
- Edsall, J. T., & Wyman, J. (1958) *Biophysical Chemistry*, Vol. 1, pp 478–483, 657, Academic Press, New York.
- Esmann, M. (1994) *Biochemistry* 33, 8558–8565.
- Esmann, M., & Skou, J. C. (1983) *Biochim. Biophys. Acta* 748, 413–417.
- Faller, L. D., Diaz, R. A., Scheiner-Bobis, G., & Farley, R. A. (1991) *Biochemistry* 30, 3503–3510.
- Faller, L. D., Smirnova, I. N., Lin, S.-H., & Stengelin, M. (1994) in *The Sodium Pump: Structure, Mechanism, Hormonal Control and its Role in Disease* (Bamberg, E., & Schoner, W., Eds.) pp 593–604, Steinkopff, Darmstadt.
- Forbush, B. (1987) *J. Biol. Chem.* 262, 11116–11127.
- Garay, R. P., & Garrahan, P. J. (1973) *J. Physiol.* 231, 297–325.
- Glynn, I. M. (1984) in *Electrogenic Transport: Fundamental Principles and Physiological Implications* (Blaustein, M. P., & Lieberman, M., Eds.) pp 39–45, Raven Press, New York.
- Glynn, I. M. (1985) *Enzymes Biol. Membr.* 3, 65–67.
- Glynn, I. M., & Karlsh, S. J. D. (1990) *Annu. Rev. Biochem.* 59, 180–185.
- Glynn, I. M., Howland, J. L., & Richards, D. E. (1985) *J. Physiol.* 368, 453–469.
- Grell, E., Warmuth, R., Lewitzki, E., & Ruf, H. (1991) in *The Sodium Pump: Recent Developments* (Kaplan, J. H., & De Weer, P., Eds.) pp 441–445, The Rockefeller University Press, New York.
- Grell, E., Warmuth, R., Lewitzki, E., & Ruf, H. (1992) *Acta Physiol. Scand.* 146, 213–221.
- Grell, E., Lewitzki, E., Ruf, H., & Doludda, M. (1994) in *The Sodium Pump: Structure, Mechanism, Hormonal Control and its Role in Disease* (Bamberg, E., & Schoner, W., Eds.) pp 617–620, Steinkopff, Darmstadt.
- Karlsh, S. J. D. (1980) *J. Bioenerg. Biomembr.* 12, 111–136.
- Karlsh, S. J. D., & Yates, D. W. (1978) *Biochim. Biophys. Acta* 527, 115–130.
- Karlsh, S. J. D., & Stein, W. D. (1985) *J. Physiol.* 359, 119–149.
- Karlsh, S. J. D., Yates, D. W., & Glynn, I. M. (1978) *Biochim. Biophys. Acta* 525, 252–264.
- Lin, S.-H., & Faller, L. D. (1993) *Biochemistry* 32, 13917–13924.
- Monod, J., Wyman, J., & Changeux, J.-P. (1965) *J. Mol. Biol.* 12, 88–118.
- Post, R. L., Hegyvary, C., & Kume, S. (1972) *J. Biol. Chem.* 247, 6530–6540.
- Sachs, J. R. (1967) *J. Clin. Invest.* 46, 1433–1441.
- Sachs, J. R. (1986) *J. Physiol.* 374, 221–244.
- Sachs, J. R., & Welt, L. G. (1967) *J. Clin. Invest.* 46, 65–76.
- Shani, M., Goldschleger, R., & Karlsh, S. J. D. (1987) *Biochim. Biophys. Acta* 904, 13–21.
- Shani-Sekler, M., Goldshleger, R., Tal, D. M., & Karlsh, S. J. D. (1988) *J. Biol. Chem.* 263, 19331–19341.
- Skou, J. C., & Esmann, M. (1983) *Biochim. Biophys. Acta* 746, 101–113.
- Smirnova, I. N., & Faller, L. D. (1993a) *Biochemistry* 32, 5967–5977.
- Smirnova, I. N., & Faller, L. D. (1993b) *J. Biol. Chem.* 268, 16120–16123.
- Steinberg, M., & Karlsh, S. J. D. (1989) *J. Biol. Chem.* 264, 2726–2734.
- Yamaguchi, M., & Tonomura, Y. (1979) *J. Biochem.* 86, 509–523.
- Xu, K. (1989) *Biochemistry* 28, 5764–5772.